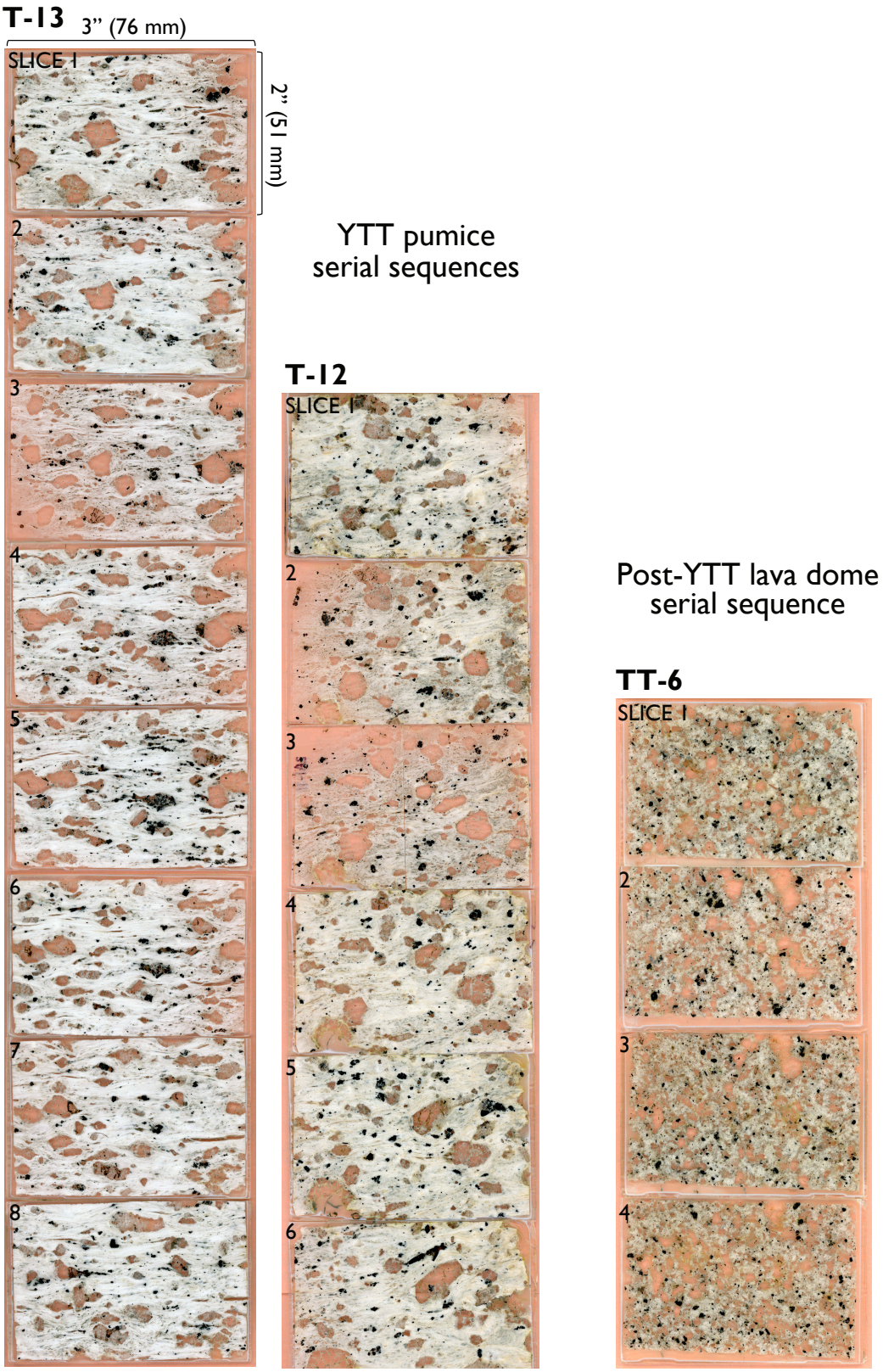

Appendix 3, Figure 1. Additional examples of serial section sequences of YTT pumice and post-YTT rhyolite lava dome samples.

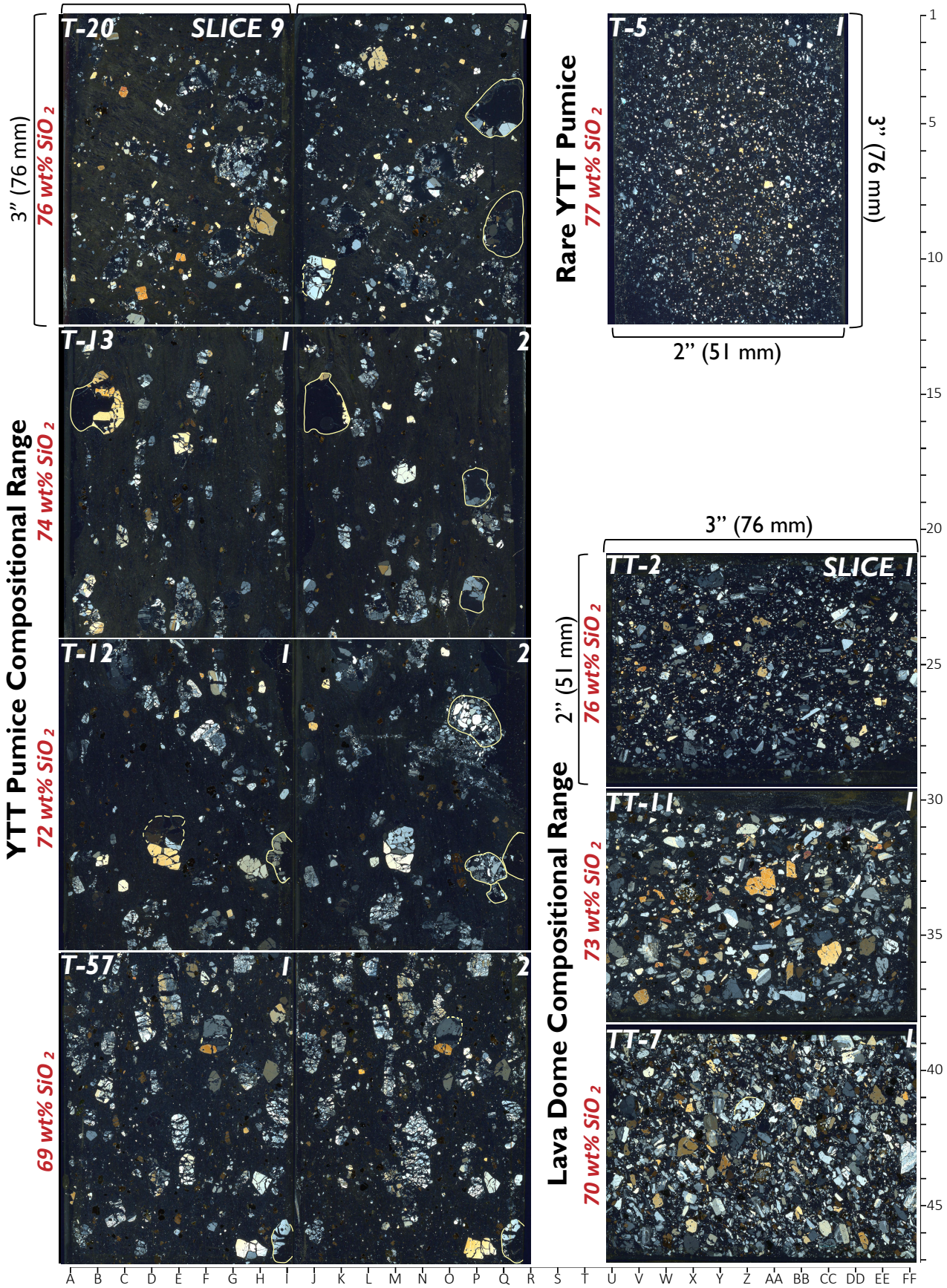

Appendix 3, Figure 2. Textures of compositionally representative YTT pumice and post-YTT lava dome samples viewed in crossed-polarized light. Samples are ordered vertically according to bulk-rock composition; two thin sections are shown of YTT pumice blocks (stretch direction oriented vertical). Most thin sections represent block edges (the first members of serial sequences), thus portions of some larger crystals are missing (solid outlines in light yellow). Dashed lines delineate optically extinct portions of large quartz. Many examples of petrographic textures discussed in the text can be located using the map grid with magnification in the digital version of this figure. Coordinates of quartz with embayments – C-8, E-10, F-38 and O-38, G-32, H-40, J-25, L-2, P-46, X-6, Y-5, Y-24, Z-33, Z-41, AA-6, AA-26, AA-27, BB-24, CC-2, CC-21, EE-36, and EE-41; optical discontinuity – A-28 and I-28, B-32, C-4, D-31 and M-31, E-7, F-38 and O-38, G-25, G-34, G-42, G-46 (note P-46 lacks discontinuity), I-26, L-8, L-21, W-7, W-5, Y-6, Y-9, Y-24, Z-6, BB-6, CC-21, and EE-26; V-shapes of contact twins in various orientations – G-34, G-42, H-26, and BB-6.

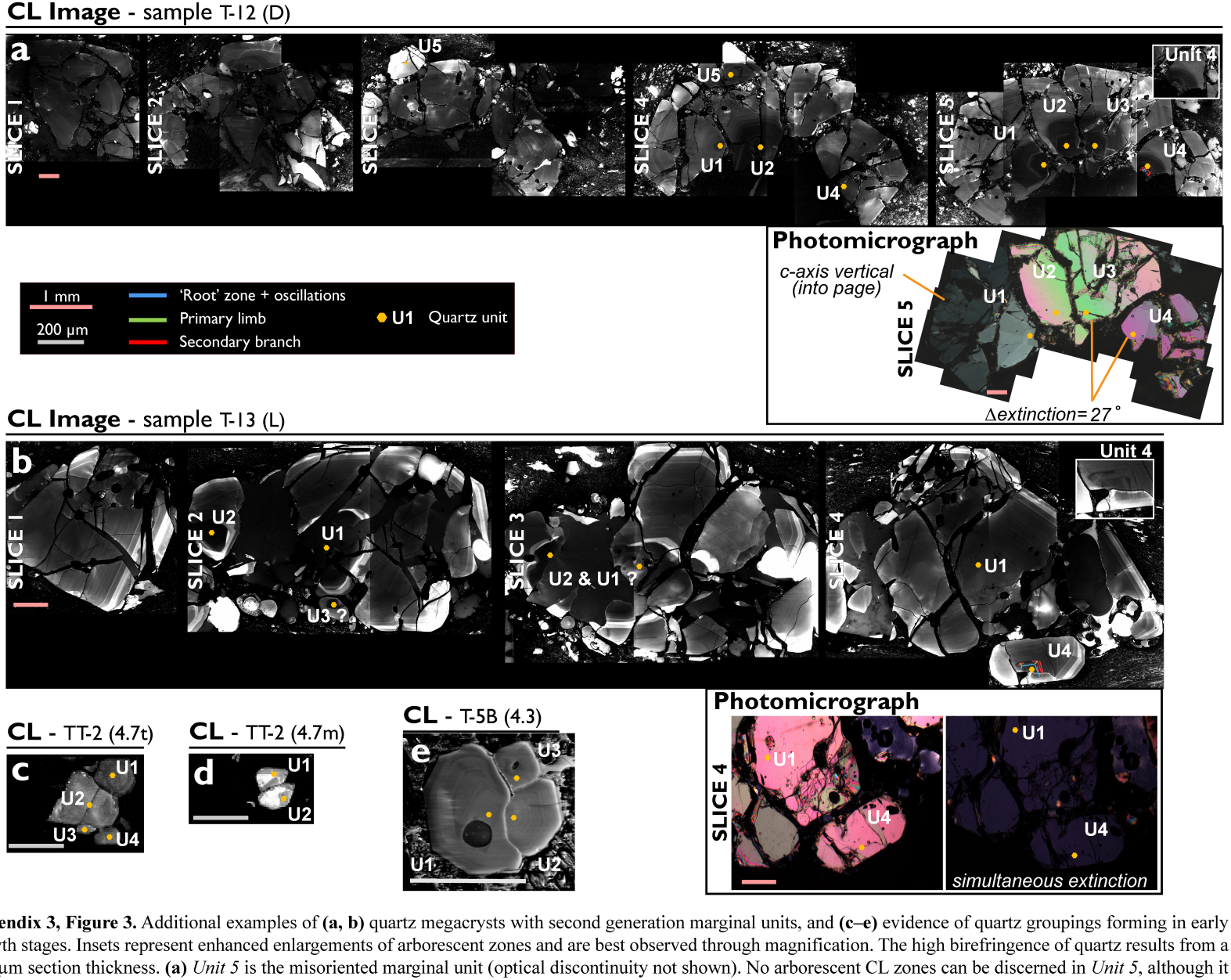

Appendix 3, Figure 3. Additional examples of **(a, b)** quartz megacrysts with second generation marginal units, and **(c–e)** evidence of quartz groupings forming in early growth stages. Insets represent enhanced enlargements of arborescent zones and are best observed through magnification. The high birefringence of quartz results from a >30 µm section thickness. **(a)** *Unit 5* is the misoriented marginal unit (optical discontinuity not shown). No arborescent CL zones can be discerned in *Unit 5*, although it contains a brighter CL core surrounded by a much darker CL zone, typical of relic hopper cores. Only *Units 2* and *3* share the same crystallographic orientation (parallel). *Units 1*, *4*, and *5* are presumed to be twinned with *Units 2* and *3*, based upon optical and EBSD data for other groupings. Crystal portions are missing due to location at the section edge. **(b)** *Unit 4* is the marginal unit that shows distinct arborescent zones at its center. The crystallographic orientation of *Unit 4* parallels those of all other units as evidenced by optical continuity and interference color. Notice that dissolution and regrowth occurred on the exterior of the entire grouping, and arborescent zones are cross cut by the newest rim zones. Some fragments were plucked. **(c)** *Units 2* and *4* are Esterel twins. *Units 1* and *3* may be related to *Unit 2* by rare twin laws, and to *Unit 4* by either multi-component twinning or through a combination of twin laws (EBSD data in Table 3 of App.[1]; also see Table 4 of App.[1]). Relative unit sizes are difficult to determine based on a single cross-section. **(d)** Two units of the same size sharing the same crystallographic orientation (EBSD data in Table 3 of App.[1]). Note their bright CL interiors. **(e)** Group of three units. *Units 1* and *2* appear to be contact twins, with *Unit 3* sitting in their re-entrant edge. *Unit 3* copies *Unit 2*'s orientation, and thus is also twinned with *Unit 1*.

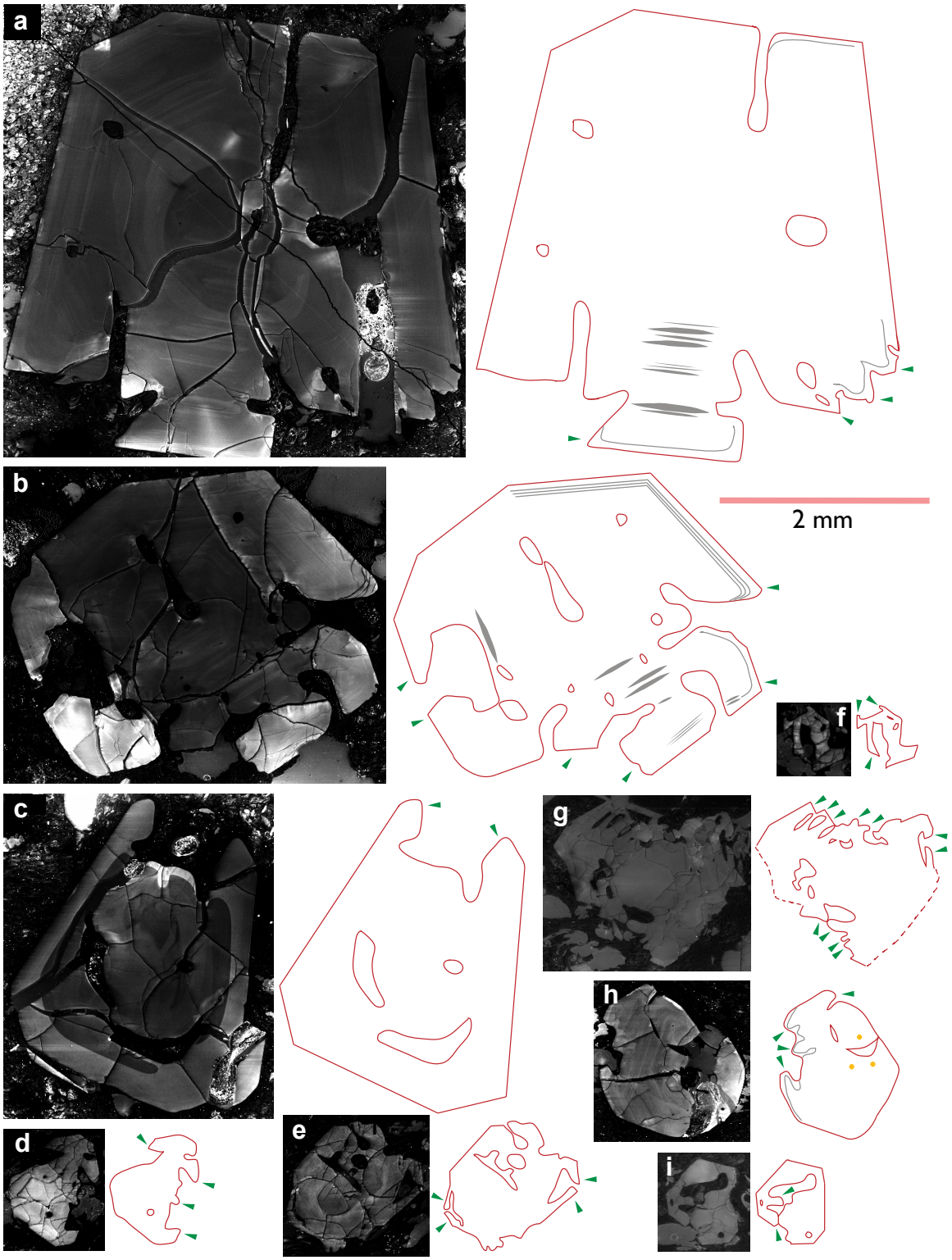

Appendix 3, Figure 4. Examples of protuberances and CL zone adaptations to embayments. Solid green arrows indicate skeletal protuberances that are more pronounced compared to those indicated by open green arrows (next page). Some CL zones are sketched to emphasize adaptation to embayment walls. Broken crystals are drawn reassembled; dashed lines indicate broken surfaces. Open fractures should not be confused with embayments. **(a)** Crystal having both polyhedral and skeletal morphology (sample T-12). The faceted hammer-head feature protruding into the matrix is characteristic of skeletal growth (cf. Fig. 10b of Swanson and Fenn 1986). **(b)** This section intersects only some skeletal cavities (T-20). Protuberances resemble pinching appendages (large overhanging terraces) when the section plane is nearly perpendicular to face directions. **(c)** Similar to (b), but some cavities appear closed in this section (T-57). **(d)** Skeletal morphology defined by hollow cavities with protrusions or terraces (TT-2). **(e)** Similar to (d), showing single terraces or growth steps above hopper cavities (TT-2). Wavy features of the crystal margin are also interpreted to be growth-related. **(f)** Protrusions similar to crystals in (d, e) (TT-2). **(g)** Poorly-zoned skeletal crystal with a number of cavities, some of which show multiple overhanging terraces (TT-10). **(h)** Similar appearance to (d); infilling of the skeletal cavity is indicated by crystal zoning (T-13). Growth steps were more defined (gray line) prior to rim growth. **(i)** Poorly-zoned crystal withskeletal-polyhedral morphology (TT-10).

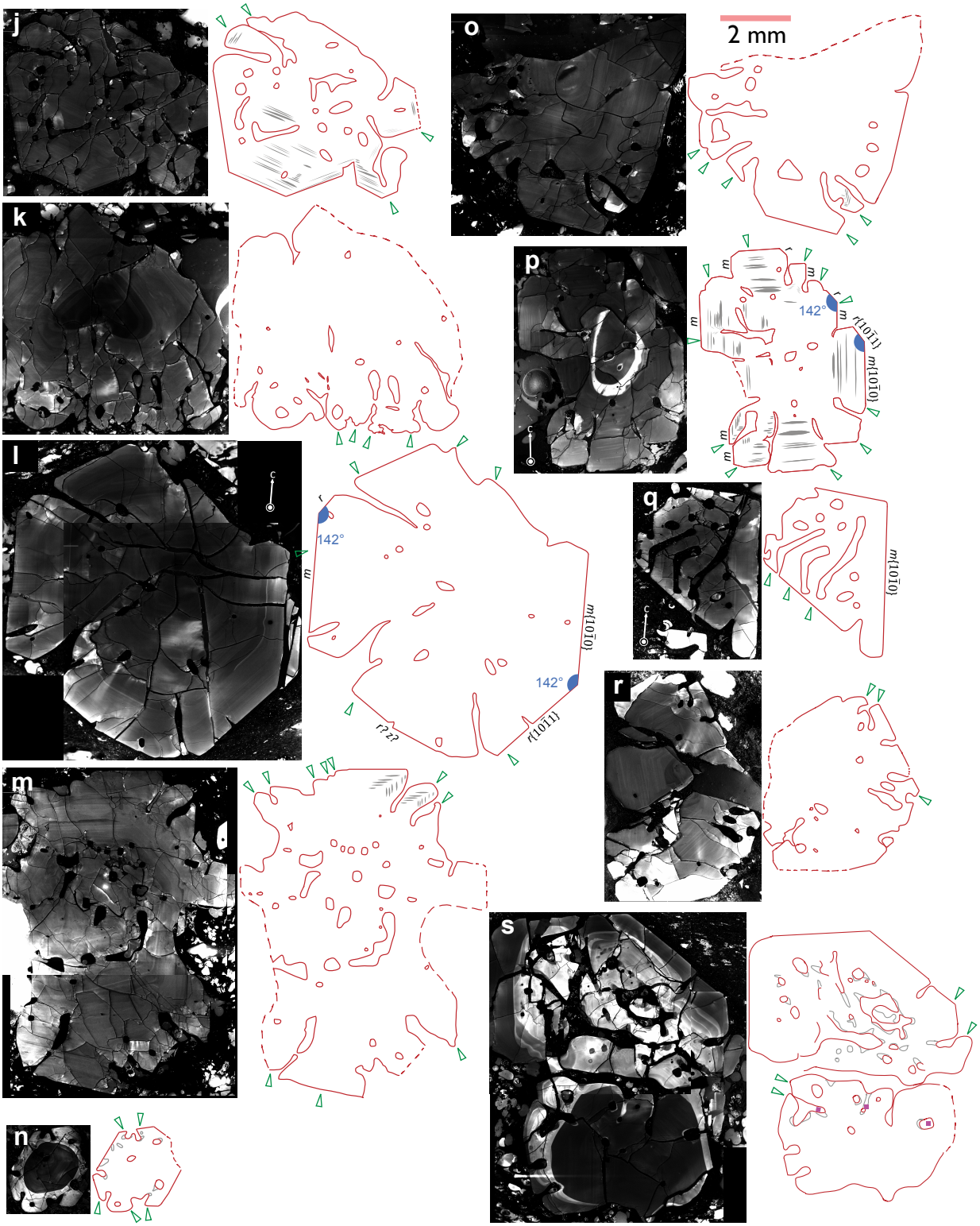

Appendix 3, Figure 4 continued. **(j)** Crystal displaying both faces and faceted protuberances (TT-10). Face directions of protuberances parallel those of the main part of the crystal. Oscillating lens zones parallel protuberance faces, and pinch out near embayment walls inside the crystal. **(k)** Embayed/jagged exterior showing faint zone adaptations and seam MIs along protuberance sutures (TT-10). **(l)** Concentric zoning displaying broad adaptations to embayments (T-13). **(m)** Convolute zoning around MIs and embayments related to at least two episodes of unstable growth (TT-9). Zone adaptations occur within protuberances that have facets in mutual orientations. **(n)** Protuberances are faceted, but show slightly rounded corners or edges (T-57). Gray lines represent post-embayment crystallization boundaries and delineate early protuberance morphologies. **(o)** Faceted protuberances with both oscillatory lens zone and concentric zone adaptations (TT-6). Appendages on the left appear sutured. **(p)** Faceted segments, or protuberances, showing conspicuous adaptation of oscillatory lens zones, which parallel protuberance face directions (TT-3). **(q)** Another section of (l) representing a cut near the crystal margin. The multiple boomerang-shaped embayments in mutual orientation indicate a crystallographic control on embayment location; these embayments may represent cavities separated by large growth ledges (terraces). **(r)** Pinching protuberances occur at the top of the image; one resembles the hammer-head feature in (a) (T-20). Oscillatory lens zones terminate near embayment walls. **(s)** Spongy texture (T-13). Zone adaptations occur around wormy embayments and MIs concentrated in the bright CL mantle. Post-entrapment crystallization occurs in embayments (gray outlines) and can be matched to the CL stratigraphy of the crystal exterior. Dissolution may have occurred preferentially along pre-existing embayments. Some pre-existing MIs in the dark core were unsealed during dissolution (rounding) and subsequent growth of the bright CL mantle. Pink squares indicate MIs cross cut by the dissolution surface in this section, which simulates the appearance of a "melt embayment".

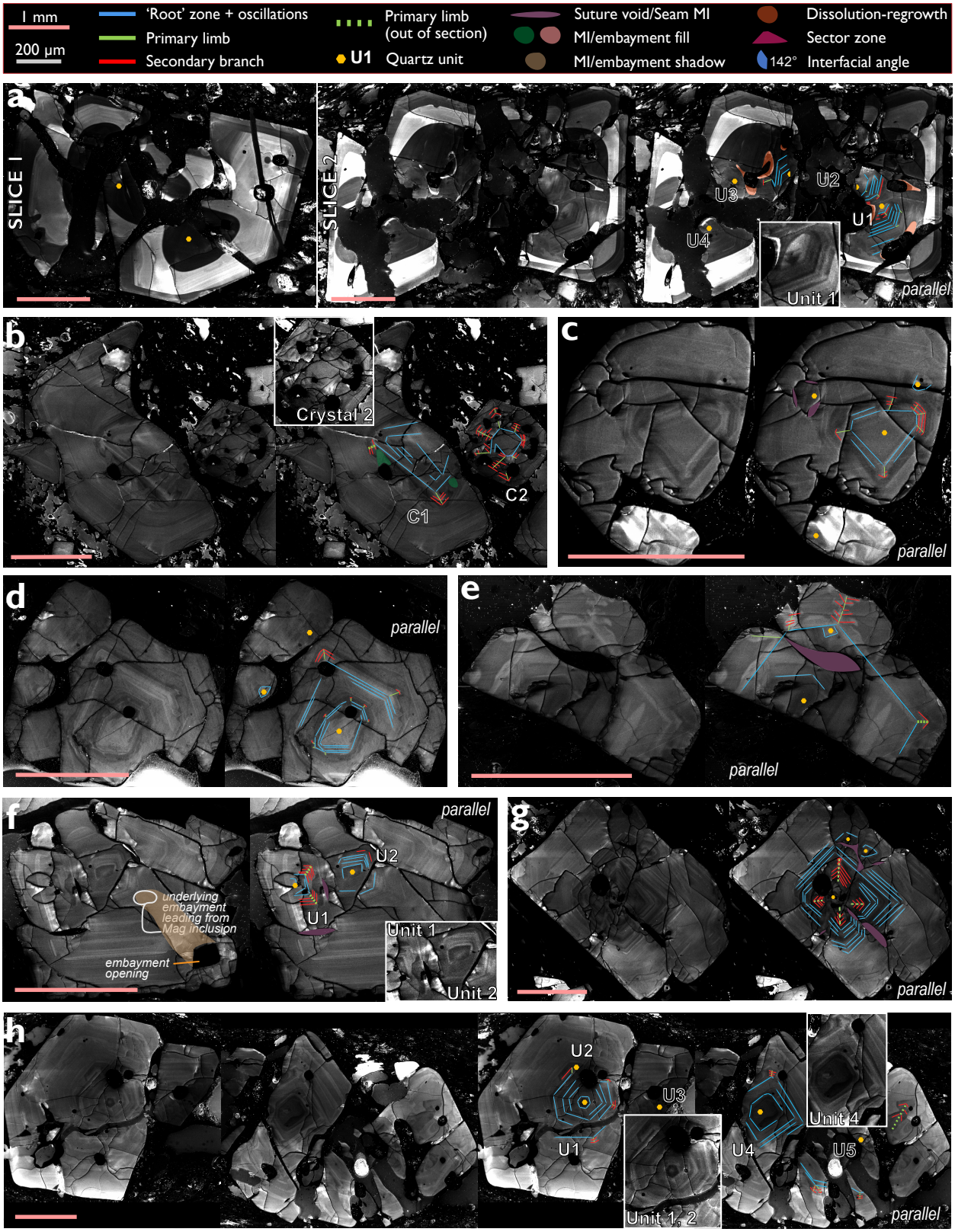

Appendix 3, Figure 5. Additional examples of arborescent CL zones. Zones can be subtle and may be better observed by magnifying the digital version of the figure. Insets represent enhanced enlargements. **(a)** Shattered group of four formerly intact parallel units (partially plucked; sample T-57). Only some units display branching patterns in *Slice 2*; *Slice 1* is shallower and does not show these features. Arborescent zones of *Unit 1* appear cross-cut, but continuous zoning occurs between *Units 1* and *2*. Embayment and crystal exterior stratigraphy match, indicating embayments were unsealed during dissolution (rounding) and subsequent growth of the thick bright CL exterior zone. **(b)** Two separate crystals exhibiting arborescent zones (SF-3). *Crystal 1* is a fragment. Melt inclusions occur between arborescent limbs and branches in both *Crystals 1* and *2*. **(c)** Four units more or less disguised as a single crystal with an embayment (TT-4). This section exposes arborescent zones in only the central unit. **(d)** The central unit displays multiple generations of 'tipped' polyhedral 'root' zones, whereas other units do not show these features in this section (TT-2). **(e)** A 'root' zone with arborescent tips encompasses two units separated by a suture void (TT-10). **(f)** Two units sectioned at nearly equivalent levels (cores). Units are bounded by a seam MI and faint suture boundary (TT-2). **(g)** Example of oscillating bright and dark zones occurring outside the branching pattern (TT-6). **(h)** Ruptured group of five parallel units with arborescent zones within cores or mantles (T-13). The interpenetration, parallel orientation, and mutual bright zone of *Units 1* and *2* are important (i.e. they share the same arborescent framework).

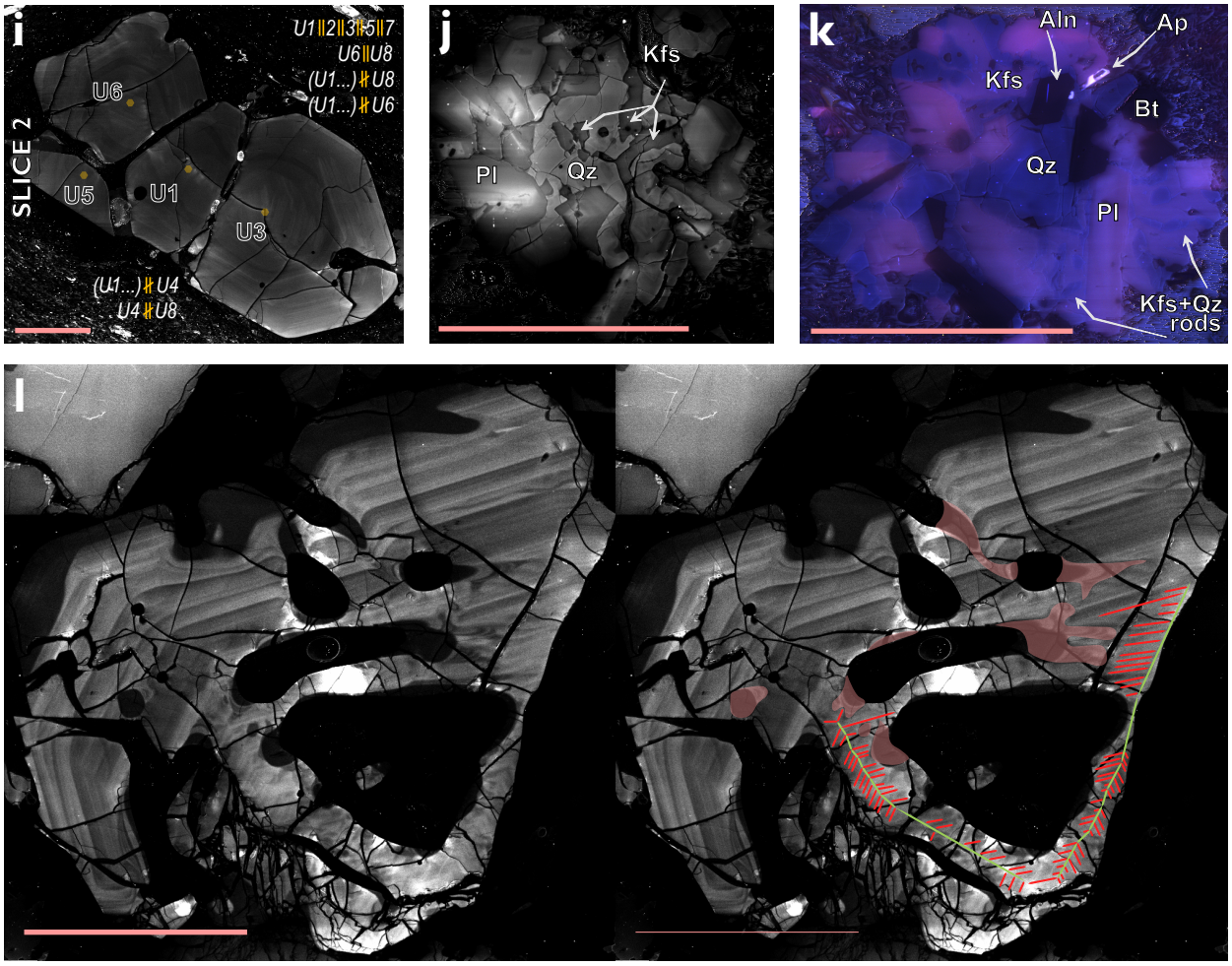

Appendix 3, Figure 5 continued. (i) *Slice 2* following *Slice 1* of Fig. 11c. *Slice 2* is a deeper section that does not expose arborescent zones observed in *Slice 1*. **(j)** Example of quartz zoning in a granophyric intergrowth (T-5B). **(k)** Color CL image showing transition from coarse to radiating quartz in a granophyric intergrowth (T-5B). Quartz is bluish; plagioclase is typically euhedral-subhedral and brightest pink; potassium feldspar is mostly anhedral and purple-pink; dark crystals are biotite or magnetite; apatites are highly luminescent, acicular, and can occur as inclusions. **(l)** Crystal fragment with embayments and crystal ledges overhanging a large triangular-shaped cavity. Arborescent zones occur just outside cavity margins, and are associated with high CL intensity zoning. Arborescent zones are still brighter than adjacent zones (SF-1). Also notice zone adaptations to embayments.

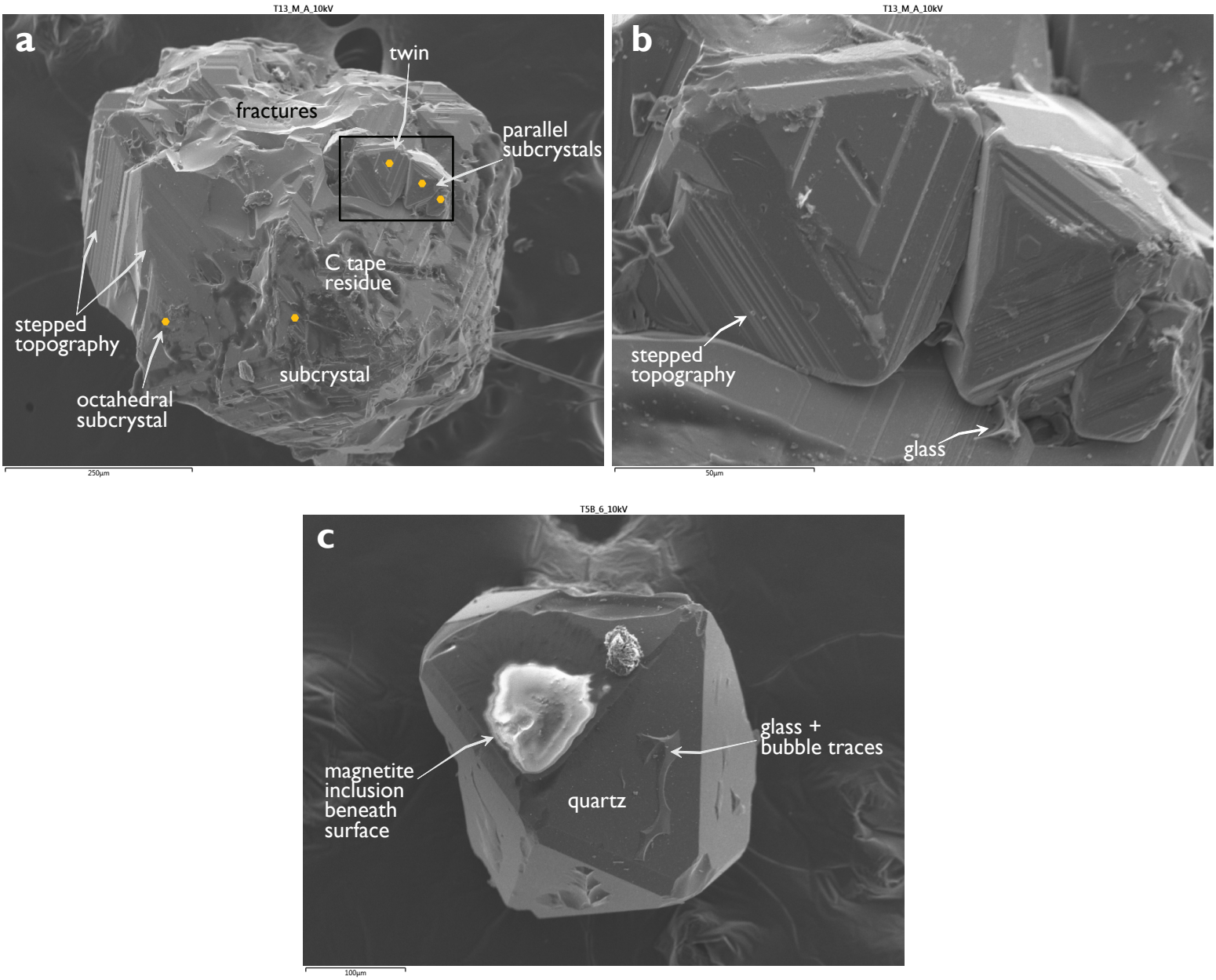

Appendix 3, Figure 6. Secondary electron images of titanomagnetite. **(a)** Stepped topography of octahedral magnetite may be due to epitaxial layers or twinning (Drev et al. 2013) (Sample T-13). Carbon tape residue obscures two large parallel units. Smaller subcrystals and a twin are enlarged in **(b)**. **(c)** Quartz crystal containing a magnetite inclusion just beneath the crystal surface. Electron interaction with the inclusion is presumably responsible for the bright area (sample T-5B).